Structural Studies of the Monolayers and Bilayers Formed by a Novel Cholesterol–Phospholipid Chimera

ARTICLE *in* LANGMUIR · JUNE 2011

Impact Factor: 4.46 · DOI: 10.1021/la200739y · Source: PubMed

6 AUTHORS, INCLUDING:

Fabrizia Foglia
Imperial College London
13 PUBLICATIONS **100** CITATIONS
SEE PROFILE

David Barlow
King's College London
131 PUBLICATIONS **3,978** CITATIONS
SEE PROFILE

Francis Szoka
University of California, San Francisco
237 PUBLICATIONS **23,893** CITATIONS
SEE PROFILE

Jayne Lawrence
King's College London
159 PUBLICATIONS **3,203** CITATIONS
SEE PROFILE

Langmuir

ARTICLE

pubs.acs.org/Langmuir

Structural Studies of the Monolayers and Bilayers Formed by a Novel Cholesterol-Phospholipid Chimera

F. Foglia,[†] D. J. Barlow,[†] F. C. Szoka, Jr.,[‡] Z. Huang,[‡] S. E. Rogers,[§] and M. J. Lawrence*[,†]

[†]Pharmaceutical Science Division, King's College London, Franklin Wilkins Building, 150 Stamford Street, London SE1 9NH, United Kingdom

[‡]Departments of Pharmaceutical Chemistry and Biopharmaceutical Sciences, School of Pharmacy, University of California at San Francisco, San Francisco, California 94143-0912, United States

[§]ISIS Facility, STFC Rutherford Appleton Laboratory, Harwell Science & Innovation Campus, Didcot, Oxfordshire OX11 0QX, United Kingdom

ABSTRACT: Langmuir isotherm, neutron reflectivity, and small angle neutron scattering studies have been conducted to characterize the monolayers and vesicular bilayers formed by a novel chimeric phospholipid, ChemPPC, that incorporates a cholesteryl moeity and a C-16 aliphatic chain, each covalently linked via a glycerol backbone to phosphatidylcholine. The structures of the ChemPPC monolayers and bilayers are compared against those formed from pure dipalmitoylphoshatidylcholine (DPPC) and those formed from a 60:40 mol % mixture of DPPC and cholesterol. In accord with previous findings showing that very similar macroscopic properties were exhibited by ChemPPC and 60:40 mol % DPPC/cholesterol vesicles, it is found here that the chimeric lipid and lipid/sterol mixture have very similar monolayer structures (each having a monolayer thickness of ~26 Å), and they also form vesicles with similar lamellar structure, each having a bilayer thickness of ~50 Å and exhibiting a repeat spacing of ~65 Å. The interfacial area of ChemPPC, however, is around 10 $Å^2$ greater than that of the combined DPPC/cholesterol unit in the mixed lipid monolayer (viz., 57 ± 1 vs 46 ± 1 $Å^2$, at 35 $mN \cdot m^{-1}$), and this difference in area is attributed to the succinyl linkage which joins the ChemPPC steroid and glyceryl moieties. The larger area of the ChemPPC is reflected in a slightly thicker monolayer solvent distribution width (9.5 vs 9 Å for the DPPC/cholesterol system) and by a marginal increase in the level of lipid headgroup hydration (16 vs 13 H_2O per lipid, at 35 $mN \cdot m^{-1}$).

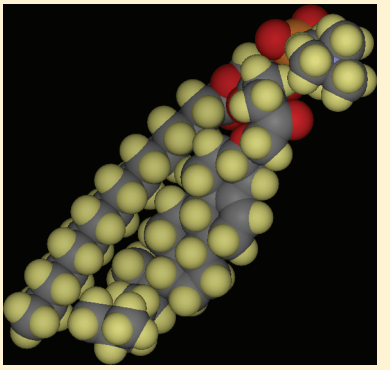

INTRODUCTION

Liposomes prepared solely from phospholipids are generally rather poor as drug delivery vehicles because they are insufficiently stable, particularly in biological milieu, and are prone to releasing their drug payload before reaching their intended target site(s).[1,2] Incorporation of cholesterol into the vesicle bilayers, however, significantly increases the vesicles' stability and makes them much less "leaky".[3] Although vesicles of this type are now often used in the formulation of chemotherapeutic drugs,[4] they nevertheless suffer significant limitations: when they are placed in biological fluids in contact with biomembranes and proteins, the cholesterol rapidly migrates from the vesicle bilayer(s) and becomes incorporated into the cell membranes.[5−7] This transfer of free cholesterol from the liposomes results in a decrease in their stability and a subsequent loss of their encapsulated contents. In order to circumvent these problems, a new category of chimeric sterol-modified phospholipid has been designed and synthesized[8] incorporating a cholesteryl moiety and an aliphatic chain, each covalently linked via a glycerol backbone to phosphatidylcholine (Figure 1). The rationale for this design is that the covalent hybridization of the sterol and phospholipid will confine the cholesteryl moiety in the lipid bilayer and thus provide improved bilayer cohesion properties and improved efficacy in drug delivery.[9]

In the studies reported here, we characterize the biophysical properties of the monolayer and vesicles formed from one of the lipids in this novel series, ChemPPC (Figure 1), and compare these interfacial structures with those involving pure phospholipid and mixtures of phospholipid with cholesterol. The earlier studies on ChemPPC demonstrated that this lipid formed vesicles with significantly less drug leakage than conventional liposomes and which were equally as effective as commercial liposomal formulations in the treatment of murine colon carcinoma.[8] Given that the properties of ChemPPC were also previously shown to approximate those exhibited by a 60/40 mol % mixture of cholesterol and DPPC,[8] it was of particular interest to compare the interfacial properties of such a mixture against those exhibited by the chimeric ChemPPC. (Note here that although the chimeric ChemPPC has one cholesteryl unit per acyl chain, comparative studies using the equivalent molar ratio of 1:1 cholesterol/DPPC cannot be performed because cholesterol levels exceeding 50 mol % lead to formation of cholesterol crystals within the membrane.)

Received: February 25, 2011
Revised: May 16, 2011
Published: June 02, 2011

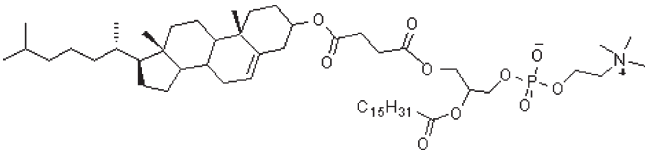

Figure 1. Chemical structure of the novel chimeric lipid, ChemPPC. (The d_{31} deuterated form has an ester-linked $C_{15}D_{31}$ chain in place of the $C_{15}H_{31}$ chain.)

EXPERIMENTAL SECTION

Materials. All chemicals were used as supplied. Fully hydrogenous 1,2-dipalmitoyl-*sn*-glycero-phosphatidylcholine (*h*-DPPC) and chain deuterated 1,2-dipalmitoyl-d_{62}-*sn*-glycero-phosphocholine (*d*-DPPC) were purchased from Avanti Polar Lipids (Alabaster, AL). Fully hydrogenous cholesterol (Chol) was obtained from Fluka (U.K.). Fully hydrogenous and palmitoyl chain deuterated versions of the lipid, ChemPPC, *h*-ChemPPC, and *d*-ChemPPC were synthesized using the method of Huang and Szoka.[8] Perdeuterated hexadecanol used for the synthesis of *d*-ChemPPC was purchased from CDN isotopes (Quebec, Canada). The purities of the isotopic forms of DPPC and cholesterol were established by determining their adsorption isotherm at the air−water interface and checking against published isotherms.[10] Wilhelmy plates used for the preparation of the Langmuir adsorption isotherms were cut from Whatman no. 1 filter paper (Merck, UK Ltd.), previously degreased by soaking in chloroform. Throughout all experiments, spectroscopic-grade chloroform (Rathburn, U.K.) and spectroscopically pure 18 MΩ·cm residual specific resistance water (Elgastat Maximapurifier, Elga U.K.) were used. All D_2O (99.9% purity) was supplied by Aldrich Ltd. (U.K.) and was used to prepare null reflecting water (nrw) of the following composition: 92% H_2O and 8% D_2O (v/v).

Surface Pressure−Area Isotherms. Monolayers of the various isotopic forms of the lipids and, in the case of DPPC, its binary mixtures with cholesterol were prepared by spreading 20 μL of a 2 mg·mL^{-1} chloroform solution of the lipids and, where appropriate, cholesterol onto the surface of clean, ultrapure water in a Nima Technologies 601 Langmuir trough (Nima Technologies, Coventry, U.K.). The trough had been previously cleaned, first using chloroform, then ethanol, and finally copious amounts of ultrapure water. Prior to compression, the monolayer films were allowed to equilibrate for 10 min to allow for complete evaporation of the chloroform. Surface pressure−area isotherms (measured in triplicate using a freshly prepared monolayer film each time) were recorded using a Wilhelmy plate suspended from a microbalance during the computer-controlled compression of the monolayer at a rate of 10−30 cm^2·min^{-1} (over any range of compression speeds, no difference has been observed in the isotherms, taking experimental error into account). The subphase was maintained at a temperature of 295 ± 2 K. For the DPPC/Chol mixture, the average area per molecule was calculated from the molar averages of the two components.

Neutron Reflection at the Air−Liquid Interface. Neutron reflectivity experiments were performed using the SURF reflectometer at the ISIS Facility (STFC Rutherford Appleton Laboratory, U.K.). Twenty microliters of various lipid mixtures in chloroform (2 mg·mL^{-1}) were added dropwise to the aqueous subphase surface in a Nima Technologies 601 Langmuir trough (Nima Technologies, Coventry, U.K.) (scrupulously cleaned according to the protocol described above). After 10 min, to allow for solvent evaporation and monolayer equilibration, the Teflon barriers of the trough were closed to compress to the required surface pressure (measured by Wilhelmy plate and microbalance). The monolayer films were compressed at a rate of 30 cm^2·min^{-1}, and a feedback mechanism employed to maintain the surface pressure at a constant preset value for the duration of the reflectivity experiment.

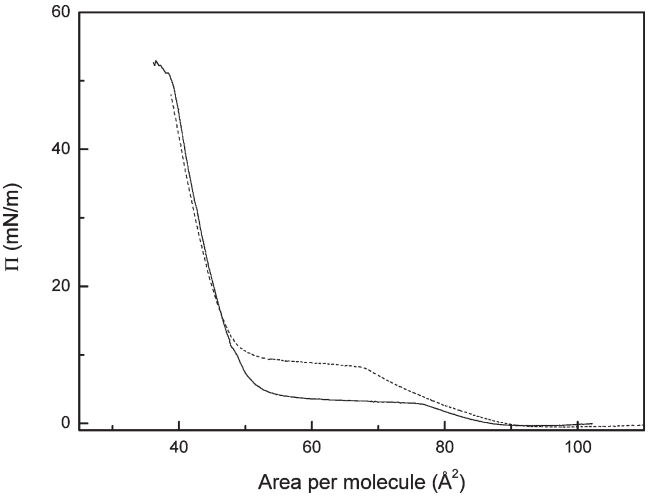

Figure 2. Langmuir (pressure−area) isotherms recorded for DPPC (solid line) and d_{62}-DPPC (dotted line).

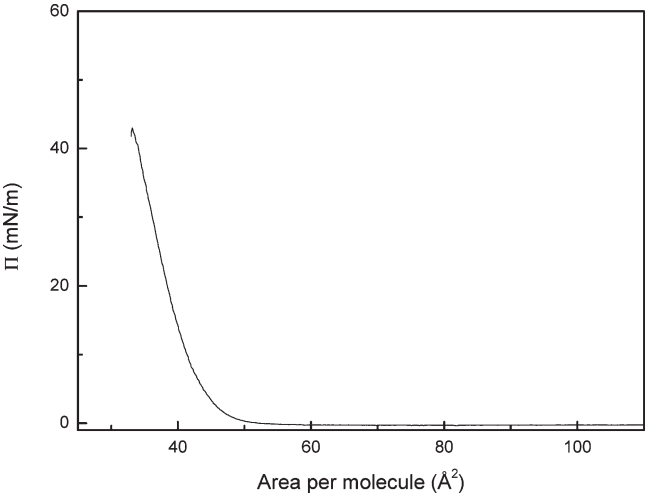

Figure 3. Langmuir (pressure−area) isotherms recorded for 60:40 mol % DPPC/Chol.

The SURF reflectometer uses a time-of-flight method to determine the wavelengths (λ) of neutrons in a white beam at a fixed angle of incidence to the monolayer surface. Measurements were made at 298 ± 0.1 K with a single detector fixed at an angle of incidence of 1.5° using a neutron λ range from 0.5 to 6.8 Å. The wavelength range covered a momentum transfer, Q, range of 0.048−0.5 Å^{-1}. As incoherent scattering is prevalent at $Q \geq 0.2$ Å^{-1}, the background scattering, which was subtracted from the experimental data before analysis, was determined by extrapolation to high Q. Reflectivity measurements were recorded for monolayers of hydrogenous and chain deuterated ChemPPC or DPPC or *h*-DPPC/Chol and *d*-DPPC/Chol (60:40 molar ratios) at surface pressures of 10, 20, 30, and 35 mN·m^{-1}.

Small-Angle Neutron Scattering (SANS). SANS measurements were performed on the LOQ beamline at the ISIS pulsed neutron source (STFC Rutherford-Appleton Laboratory, U.K.). Wavelength-dependent corrections were made to allow for the incident spectrum, detector efficiencies, and measured sample transmissions to create a composite SANS pattern. The LOQ instrument gives a Q range of 0.008−0.22 Å^{-1}. Comparisons with scattering from a partially deuterated

dx.doi.org/10.1021/la200739y |*Langmuir* 2011, 27, 8275–8281

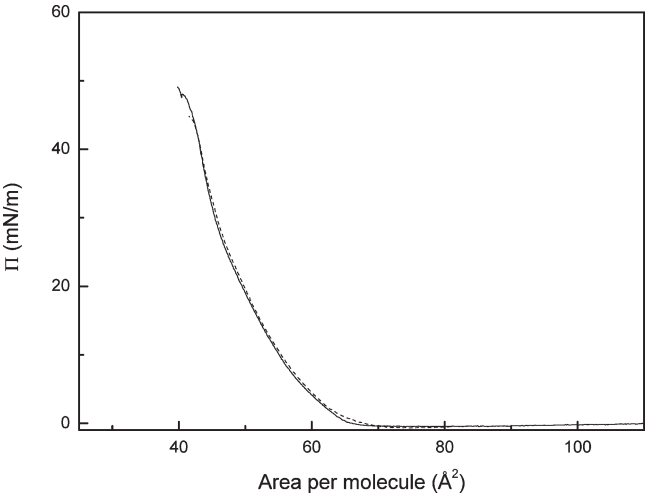

Figure 4. Langmuir (pressure−area) isotherms recorded for ChemPPC (solid line) and d_{31}-ChemPPC (dotted line).

Table 1. Sum of Atomic Scattering Lengths (b_L), Volumes (V), and Scattering Length Densities (ρ) for the Various Components of the Lipid Systems Studied

	$b_L/10^{-5}$ Å	V/Å^3	$\rho/10^{-6}$ Å^{-2}
h-DPPC	27.5	1210	0.23
d_{62}-DPPC	673.0	1210	5.56
Chol	13.2	602	0.22
d_{31}-ChemPPC	71.5	1446	0.49
h-ChemPPC	387.8	1446	2.68
D_2O	19.1	30	6.35
H_2O	−1.67	30	−0.56

Table 2. Variation in Lipid Monolayer Structure and Dimensions as a Function of Surface Pressure (π) Determined through Guinier Analyses of Neutron Reflectivity Data[a]

	60:40 mol % DPPC/Chol			DPPC			ChemPPC		
π (mN·m^{-1})	a_0	L_M	σ	a_0	L_M	σ	a_0	L_M	σ
10	47	29.4	24.0	nd	nd	nd	66	28.4	23.2
20	44	30.7	25.1	56	30.5	24.9	62	29.4	24.0
30	45	30.4	24.8	49	30.8	25.2	56	30.4	24.8
35	45	31.1	25.4	49	30.9	25.3	55	31.2	25.5

[a] Interfacial molecular areas (a_0, Å^2) are quoted with standard errors of ±1 Å^2. Monolayer slab thicknesses (L_M, Å) and Gaussian distribution widths (σ, Å) are quoted with standard errors of ±0.5 Å. (nd) The parameters for DPPC monolayers at 10 mN·m^{-1} have not been determined.

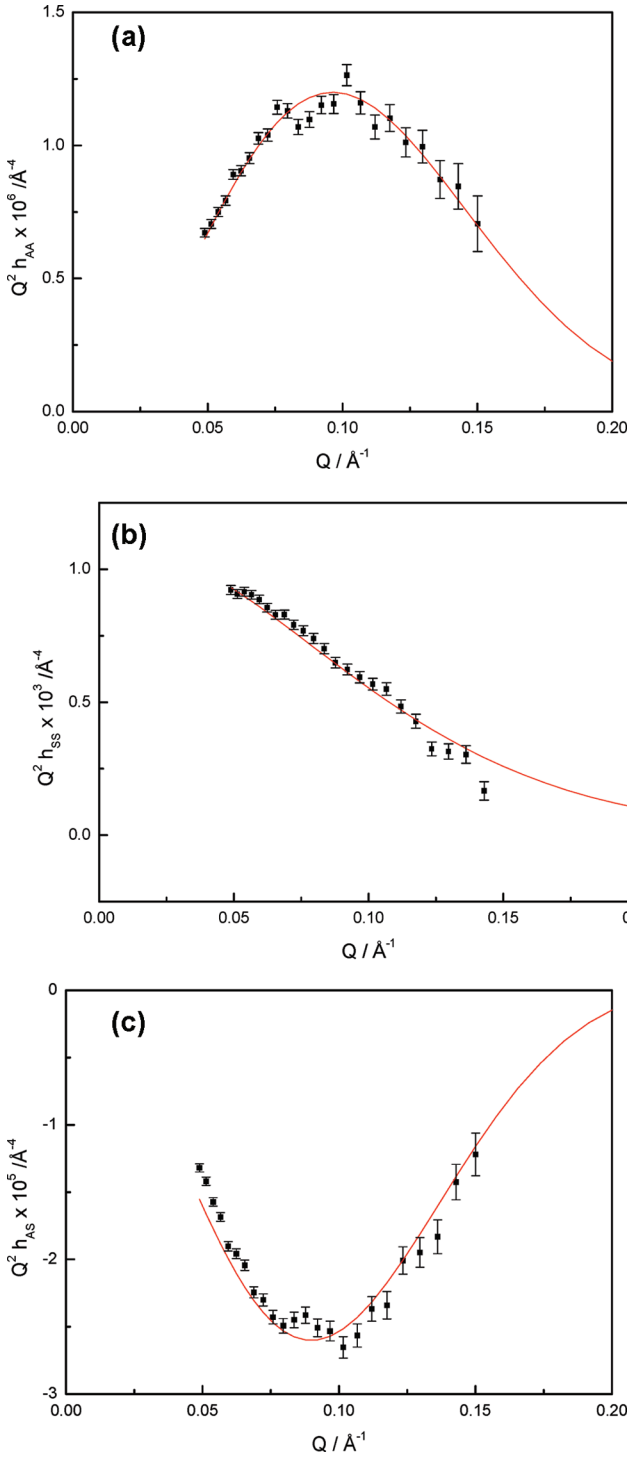

Figure 5. Plots of partial structure factors for (a) h_{LL}, (b) h_{SS}, and (c) h_{LS} against Q for the ChemPPC monolayer maintained at 35 mN·m^{-1}. h_{LL} was modeled assuming a Gaussian distribution and h_{SS} assuming a tanh distribution.

polystyrene standard allow absolute scattering cross sections to be determined, with an error of around ±2%. The vesicle samples for the SANS studies were prepared at a total lipid (or lipid−sterol) concentration of 1.25 mg·mL^{-1} by using the thin film hydration technique of Kirby and Gregoriadis[11] using D_2O for the *h*-lipid films and either H_2O or D_2O for the *d*-lipid films. These lipid dispersions were first vortexed for 5 min, placed in a water bath at 328 K for 10 min, and finally ultrasonicated for 5 min using a probe sonicator (Lucas Dawes Ultrasonicator Soniprobe). After sonication, the suspensions were centrifuged at 12 000 rpm for 2 min (MSE Micro Centaur, Sanyo, U.K.) to remove any titanium particles shed by the sonicator probe. The vesicles were allowed to anneal at room temperature for at least 1 h prior to any experimental treatment. Vesicle suspensions were placed in scrupulously cleaned, disk-shaped fused silica cells (Hellma, U.K., Ltd., Essex) of path length

dx.doi.org/10.1021/la200739y |*Langmuir* 2011, 27, 8275–8281

Table 3. Variation in Lipid Monolayer Structure and Dimensions as a Function of Surface Pressure (π) Determined through Partial Structure Factor Analyses of Neutron Reflectivity Data[a]

	60:40 mol % DPPC/Chol				DPPC				ChemPPC			
π (mN·m^{-1})	a_0	σ_L	σ_S	δ	a_0	σ_L	σ_S	δ	a_0	σ_L	σ_S	δ
10	48	23.9	9.8	12.0	nd	nd	nd	nd	69	24.5	9.0	12.3
20	45	24.7	8.6	13.0	58	23.2	9.8	14.5	66	24.6	9.0	13.0
30	46	25.3	8.7	13.5	52	23.4	9.0	14.5	59	25.5	9.2	14.0
35	46	25.4	9.0	14.0	51	23.6	9.3	16.0	57	26.0	9.5	14.0

[a] Interfacial molecular areas (a_0, Å^2) are quoted with standard errors of ±1 Å^2. Lipid and solvent layer distribution widths and the separations between the distribution midplanes (σ_L, σ_S, and δ, respectively, in Å) are quoted with standard errors of ±0.5 Å. (nd) The parameters relating to DPPC at 10 mN·m^{-1} have not been determined.

1 mm (for H_2O) or 2 mm (for D_2O). Using a 12 mm diameter neutron beam, SANS measurements were carried out at 298 ± 0.1 K. Backgrounds from pure H_2O and pure D_2O were subtracted. All fitting procedures included flat background corrections to allow for any mismatch in the incoherent and inelastic scattering between the sample and solvents. Fitted background levels were always checked to ensure that they were of a physically reasonable magnitude. Dynamic light scattering measurements (Brookhaven Zeta plus potential analyzer, Stockwood, U.K.) gave apparent vesicle sizes of ∼100 nm for the ChemPPC vesicles, ∼120 nm for the DPPC vesicles, and ∼130 nm for the 60/40 mol % DPPC/Chol vesicles. The vesicles (prepared at the same concentrations as used for SANS studies) were stable for at least 3 days, showing no significant change in particle size or polydispersity over this period.

As SANS data for each system were obtained using three different H/D contrasts provided by *h*-lipid vesicles dispersed in D_2O and *d*-lipid vesicles dispersed in D_2O or H_2O, the data were simultaneously fitted using an infinite planar sheet and one-dimensional paracrystalline stack model[12−14] that we have used previously for modeling vesicle SANS data,[15−17] with parameters optimized using Heenan's FISH software.[18] The parameters refined in the model fitting included the sample background scattering, the volume fractions of unilamellar vesicles (ULVs) and multilamellar vesicles (MLVs), the thickness of the vesicle lamellae (L_V, Å; taken to be the same for the ULVs and MLVs), and the *d*-spacing of the MLVs (D, Å). Four other parameters involved in the SANS models were initially treated as adjustable (and were thus fitted along with the five parameters listed above), but preliminary analyses revealed that their fitted values showed insignificant variation from data set to data set; in the final analyses, therefore, these parameters were constrained as fixed. These fixed parameters (and their constrained values) included the polydispersity on the thickness of the vesicle lamellae ($\sigma(L_V)/L_V$; taken as zero, but of practical necessity input as 10^{-6}), the polydispersity on the MLV *d*-spacing ($\sigma(D)/D$; 0.05), the mean lamellarity of the MLVs (M; 4), and the Lorentz correction factor ($R\sigma$, 240 Å).

RESULTS AND DISCUSSION

Surface−Pressure Area (π−A) Isotherms. The isotherms recorded for *h*-DPPC (Figure 2, solid line) were wholly consistent with those reported by previous workers[10] and indicate that the lipid film exhibits an expanded phase at large areas per molecule, a_0 (beyond ∼90 Å^2), a transitional phase at intermediate a_0 (approximately ∼77 and ∼60 Å^2), and a condensed phase at a_0 less than ∼50 Å^2. As expected (given the known effects of deuteration on lipid phase transition[19−21]), the isotherms recorded for the d_{62}-DPPC monolayers (dotted line, Figure 2) showed significant differences in the domain corresponding to the film's transition from an expanded to a condensed phase (with the onset of the phase transitions for the *h*-DPPC and d_{62}-DPPC occurring at a_0 ∼77 and ∼67 Å^2, respectively), but otherwise overlaid the isotherm for the *h*-lipid very well, with no significant differences evident for the surface pressures employed in the subsequent neutron reflectivity studies.

For comparison with ChemPPC, as noted earlier, we would ideally also wish to record the isotherm for the equivalent mixture[8] of DPPC with 67 mol % free cholesterol. It is well established, however, that in films having this composition the molecules are demixed giving DPPC-rich and cholesterol-rich domains, with compression of the film leading to an irreversible expulsion of sterol into the subphase.[10,22] No such study was thus attempted, and isotherms were instead recorded for a mixture involving 60:40 mol % DPPC/Chol. As would be expected, these isotherms (Figure 3) were very different from those obtained for DPPC alone, showing no discernible phase transition, and with the film passing almost immediately from a gaseous phase to a condensed phase at a_0 of ∼50 Å^2. Consistent with all previous reports, therefore, it is clear that the cholesterol abolishes the abrupt transition from the expanded to condensed phase film observed for pure DPPC monolayers.[10]

As with the DPPC/Chol system, the ChemPPC isotherms (Figure 4) show no evidence of a phase transition, suggesting that the presence of the cholesteryl moeity as part of the lipid hydrophobe abolishes the phase transition due to the hexadecanoyl chain on position 2. Interestingly, however, the film was much more expanded than that measured for the 60:40 mol % mixture of DPPC and cholesterol, with the ChemPPC film remaining in an expanded state from the liftoff area at ∼52 Å^2 until its collapse at a surface pressure of around 47 mN·m^{-1}. No difference was noted between the isotherm obtained for the two isotopic forms of ChemPPC (Figure 4), which is as would be expected given the absence of any phase transition in the compressed film. We note too that there was no evidence of hysteresis in the isotherms produced on compression and decompression of the ChemPPC film, and that the limiting area per molecule for the lipid (extrapolated from the curve at the onset of collapse) is around 55−60 Å^2, which compares with ∼50 Å^2 for pure DPPC and ∼45 Å^2 for the 60:40 mol % DPPC/Chol mixture.

Neutron Reflection. Neutron reflectivity measurements were recorded for monolayers of DPPC, ChemPPC, and DPPC mixed with 40 mol % cholesterol, at surface pressures of 10, 20, 30, and 35 mN·m^{-1}. For each system, three different H/D contrasts were employed, involving *d*-lipid on nrw, *d*-lipid on D_2O, and *h*-lipid on D_2O.

For each of the *d*-lipid systems spread as monolayers on nrw, the measured reflectivity, $R(Q)$, arises predominantly from the

dx.doi.org/10.1021/la200739y |*Langmuir* 2011, 27, 8275–8281

adsorbed layer, and so when the data are transformed[23] as $\ln(Q^2R(Q))$ vs Q^2, the slope of the fitted regression line, $\tan(\theta)$, yields an estimate for the second moment of the thickness of the distribution of the deuterated component (i) of the lipid layer, σ_i

$$\tan(\theta) = -\sigma_i^2 \quad (1)$$

and the intercept on the ordinate (ι) gives the surface excess of the adsorbed species, Γ:

$$\iota = \ln(16\pi^2 b_L \Gamma) \quad (2)$$

where b_L is the sum of the atomic scattering lengths for the adsorbed species (Table 1). From Γ, we can determine the lipid interfacial molecular area, $a_0 = (\Gamma N_a)^{-1}$ (where N_a is Avogadro's number). On the assumption that the adsorbed layer is adequately modeled as an infinite flat sheet, we can also derive the slab thickness of the deuterated lipid component as

$$L_M = \sqrt{12}\sigma_i \quad (3)$$

and if we consider instead a Gaussian distribution for the volume fraction profile of the lipid component, the width of this Gaussian is obtained as

$$\sigma = \sqrt{8}\sigma_i \quad (4)$$

Since the deuteration here is confined just to the hydrophobes of the various lipids studied, it is the thickness of the hydrophobe layers that are provided by these Guinier analyses, rather than the full thickness of the lipid layer (with the neutron scattering length of the *h*-lipid headgroup being appreciably smaller than that for the deuterated hydrophobe, viz. 60×10^{-5} vs 311×10^{-5} Å). The complete set of values derived for L_M, σ, and a_0 are summarized in Table 2.

For DPPC, the data (Table 2) show, as expected, that the monolayer thickness increases with increasing surface pressure, with L_M rising from ~28 Å at 10 mN·m^{-1} up to ~31 Å at 35 mN·m^{-1}. Given that the fully extended length of a DPPC molecule is ~30 Å, it is clear that at the lower surface pressures the lipid molecules must be a little disordered and/or tilted slightly with respect to the interface normal. As the surface pressure is increased, the extent of this tilt decreases and/or the roughening of the adsorbed layer increases. These changes in the adsorbed layer are accompanied by a decrease in the molecular interfacial area, with a_0 decreasing from ~56 Å^2 at 20 mN·m^{-1} down to ~49 Å^2 at 35 mN·m^{-1}.

In the case of ChemPPC, the data (Table 2) again show the expected increase in layer thickness, with the thickness estimates obtained at each of the four surface pressures being virtually identical to the corresponding estimates obtained for DPPC. The novel lipid's interfacial molecular area likewise decreases when the surface pressure increases, but the change here (compared against that seen with DPPC) is much less marked, with the ChemPPC giving a_0 values of 62 Å^2 at 20 mN·m^{-1} and 55 Å^2 at 35 mN·m^{-1}.

For the 60:40 mol % DPPC/Chol mixture, the changes seen in the film thickness are much the same as those seen for both the pure DDPC and the ChemPPC films (remaining around 31 Å between 20 and 35 mN·m^{-1}). There is very little change in a_0 as a function of surface pressure, however, such that a_0 is more or less constant at 44−45 Å^2 over the range 20−35 mN·m^{-1} (Table 2). Moreover, if we compute the weighted mean interfacial area for the more compressed DPPC/Chol film, the area so obtained is the same as measured experimentally, namely, $(0.6 \times 49) + (0.4 \times 38) \approx 45$ Å^2, indicating that there is no condensing

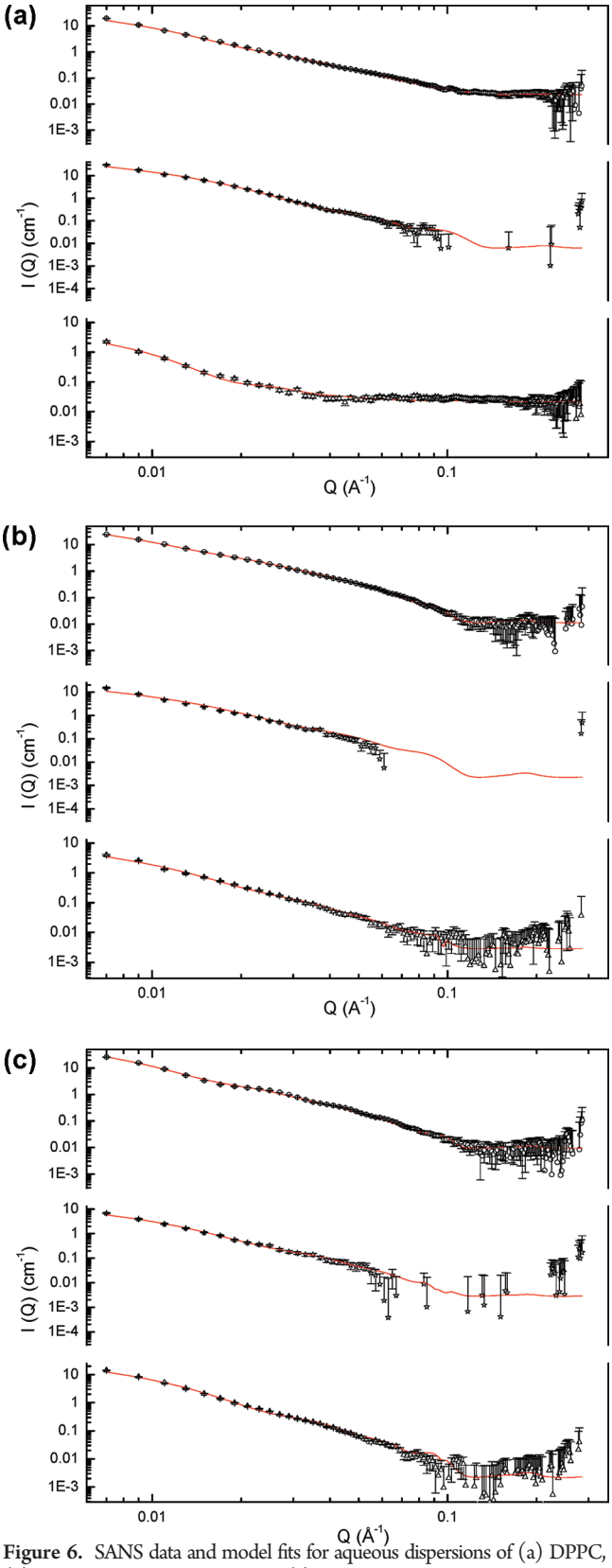

Figure 6. SANS data and model fits for aqueous dispersions of (a) DPPC, (b) 60:40 mol % DPPC/Chol, and (c) ChemPPC vesicles. The upper panel in each case shows the data obtained for the *h*-lipid in D_2O, while the center and lower panels show the data for the *d*-lipid in H_2O and D_2O, respectively. $I(Q)$ are scattering intensities, and Q is the neutron momentum transfer, in Å^{-1}. The structural parameters for the (simultaneous) model fits shown are presented in Table 4.

dx.doi.org/10.1021/la200739y |*Langmuir* 2011, 27, 8275–8281

Table 4. Structural Parameters Obtained through Model Fitting of SANS Data Recorded for the DPPC, 60:40 mol % DPPC/Chol, and ChemPPC Lipid Vesicle Dispersions[a]

			h-lipid in D_2O		*d*-lipid in D_2O		*d*-lipid in H_2O	
	L (Å)	*D* (Å)	*M*	ULV/MLV	*M*	ULV/MLV	*M*	ULV/MLV
ChemPPC	50.9 (0.3)	65.1 (0.2)	6	1.99	4	1.18	4	1.8
DPPC	42.9 (0.4)	57.4 (0.4)	5	2.80	6	0.66	3	0.98
60:40 mol % DPPC/Chol	49.3 (0.3)	67.3 (0.3)	6	5.56	4	2.46	4	1.96

[a] *L* is the vesicle bilayer thickness (in Å), *D* is the lamellar *d*-spacing (in Å), *M* is the mean lamellarity of the multilamellar vesicles, and ULV/MLV gives the relative proportion on unilamellar and multilamellar vesicles in the samples. Values in parentheses show the standard errors on the fitted parameters.

effect caused by the cholesterol in this mixture (as has been noted by previous researchers[24]).

In order to provide for a more detailed modeling of the various lipid monolayer structures, the measured data were remodeled in terms of partial structure factors assuming a kinematic approximation[25] (and employing the molecular volumes, atomic scattering lengths, and scattering length density data as shown in Table 1). The reflectivity of the layer, $R(Q)$, was taken as a function of the atomic scattering lengths of the lipid(s) (b_L) and solvent (b_S)

$$R(Q) = \frac{16\pi}{Q^2}\{b_L{}^2 h_{LL} + b_S{}^2 h_S + 2b_L b_S h_{LS}\} \quad (5)$$

where h_{ii} and h_{ij} are the partial structure factors given by

$$h_{ii}(Q) = |n_i(Q)|^2 \; h_{ij}(Q) = Re|n_i(Q)\cdot n_j(Q)| \quad (6)$$

with $n_i(\kappa)$ being the 1D Fourier transforms of $n_i(z)$, the mean number density profiles of component i along the interface normal (z)

$$n_i(Q) = \int_{-\infty}^{\infty} \exp(-iQz)\; n(z)\; dz \quad (7)$$

The number density distributions, $n_L(z)$, for the lipid(s) were modeled as Gaussian distributions

$$n_L(z) = n_0 \exp\left(-4\frac{z^2}{\sigma^2}\right) \quad (8)$$

where n_0 is the number density at the distribution center and σ is its width at height n_0/e. For the distribution of water across the interface, a tanh function was used

$$n_S(z) = n_{SO}\left\{\frac{1}{2} + \left[\frac{1}{2}\tanh\left(\frac{z}{\sigma_S}\right)\right]^{-1}\right\} \quad (9)$$

where n_{SO} is the number density for bulk water and σ_S is the width of the distribution. The distances, δ, separating the midplanes of the lipid and solvent distributions were obtained as

$$h_{LS}(Q) = \pm (h_{LL}h_{SS})^{1/2} \sin(Q\delta) \quad (10)$$

Representative data from the partial structure factor analyses of the ChemPPC system are shown in Figure 5, and the complete set of derived values for a_0, σ_S, σ_L, and δ for all the systems studied are summarized in Table 3.

In general, the structure factor analyses yield a_0 and σ_L values that are reasonably consistent with the estimates obtained via the (more approximate) Guinier analyses (cf., Tables 2 and 3). In addition, the structure factor analyses provide information on the distribution of solvent within the lipid monolayers. For all three of the lipid systems, the solvent layer seems to be about 9−10 Å thick, which is much the same as has been reported for DSPC monolayers.[26] There is a marginal thinning of the layer with increased surface pressure in the case of the DPPC and DPPC/Chol films, but it remains at more or less constant thickness with changing surface pressure (at ∼9 Å) in the case of the ChemPPC film. The separations between the midplanes of the lipid and solvent distributions vary depending upon the particular lipid system and the surface pressure. As expected (given the more pronounced surface pressure induced changes in thickness of the lipid layer), the greatest change in δ is seen for the pure DPPC film, where it varies between ∼14 Å at 20 mN·m^{-1} and 16 Å at 35 mN·m^{-1}. For both the ChemPPC and DPPC/Chol films, the separations at the higher surface pressure are somewhat lower (around 14 Å).

For the calculation of the monolayer hydration, we integrate over the number density distributions for the lipid(s) and solvent (computed according to eqs 8 and 9) and calculate the ratio of these integrals to obtain the number of water molecules associated with the lipid(s) within the defined integration limits. At the highest surface pressure of 35 mN·m^{-1}, such calculations give the hydration of the DPPC as 15 H_2O per molecule, calculated over a slab of 31 Å thickness centered at the midpoint of the lipid distribution. This figure is close to, but rather lower than, that derived on the basis of gravitometric X-ray studies on phospholipid bilayers, namely, 12−13 H_2O per lipid.[27] The corresponding values calculated for the DPPC/Chol and ChemPPC monolayers maintained at 35 mN·m^{-1} are 13 and 16 H_2O per molecule, respectively. The levels of hydration of the three lipid monolayers are quite comparable, therefore, and (with calculated uncertainties of ±0.5 H_2O) show only minor variations but nevertheless follow the trend in their respective interfacial areas, a_0 (with ChemPPC > DPPC > DPPC/Chol).

Small-Angle Neutron Scattering. For each system, the SANS data for the vesicle dispersions were obtained using three different H/D contrasts provided by *h*-lipid vesicles dispersed in D_2O and *d*-lipid vesicles dispersed in D_2O or H_2O. Simultaneous model fitting of the three curves obtained for each system (Figure 6), using the FISH[18] program, provided estimates for the thickness of the vesicle bilayer (L_V, Å), the lamellar repeat distance (*d*-spacing, *D*, Å), vesicle lamellarity (*M*), and the relative proportions of unilamellar and multilamellar vesicles in the dispersions (Table 4).

Here, it is interesting to note that although the three lipid systems produce monolayers that have very similar thickness (each being ∼31 Å thick at π = 35 mN·m^{-1}), they appear to form vesicles with rather different bilayer thickness. The 60:40 mol % DPPC/Chol mixture gives vesicles with L_V = 49 Å,

dx.doi.org/10.1021/la200739y |*Langmuir* 2011, 27, 8275–8281

while the ChemPPC and DPPC bilayers have L_V = 51 and 43 Å, respectively. In all three cases, L is less than twice the thickness of the corresponding monolayer (being 15−20% thinner), which would seem to indicate that the molecules within the two leaflets of the bilayer are significantly interdigitated/tilted, with the extent of interdigitation/tilting following the order DPPC ≫ DPPC/Chol ≈ ChemPPC.

CONCLUSIONS

A simple inspection of the chemical structure of ChemPPC might lead one to suppose that the properties of the molecule would approximate those exhibited by a 60:40 mol % mixture of cholesterol and DPPC, since such a mixture provides roughly the same ratio of sterol to C_{16} chains. Indeed, we have shown previously how, when used to prepare lipid vesicles, the osmotically induced leakage of contents from ChemPPC vesicles is very similar to that observed with 60:40 mol % DPPC/Chol vesicles.[8] It is interesting to note here, therefore, that this accords with the similarity in the structures of the ChemPPC and 60:40 mol % DPPC/Chol monolayers and bilayers. For the former, for example, we see (Table 3) that, at 35 $mN \cdot m^{-1}$, the width of the Gaussian distribution used in modeling the lipid layer is ∼26 Å for both ChemPPC and the DPPC/Chol monolayers, and the corresponding separations between the midpoints of the monolayer lipid and solvent distributions are also the same, with each being 14 Å. The vesicle lamellae of the two systems seem also very similar (Table 4), with each having a bilayer thickness of ∼50 Å and exhibiting a repeat spacing of ∼65 Å, the former being some 7 Å thinner for DPPC vesicles and the latter ∼3 Å thinner for the DPPC vesicles. The interfacial area of ChemPPC, however, is around 10 $Å^2$ greater than that of the combined DPPC/Chol unit in the (60:40 mol %) mixed lipid monolayer (viz., 57 ± 1 vs 46 ± 1 $Å^2$, at 35 $mN \cdot m^{-1}$). This difference in area clearly arises because of the succinyl linkage which joins the ChemPPC steroid and glyceryl moieties (Figure 1). The larger area of the ChemPPC is reflected in the slightly thicker monolayer solvent distribution width (9.5 vs 9 Å), and by a marginally higher level of the lipid headgroup hydration (16 vs 13 H_2O, at 35 $mN \cdot m^{-1}$).

As a corollary to these studies, therefore, we note that it is possible, to a good approximation, at least, to deduce the properties of chimeric molecules by a simple extrapolation from the known properties of the separate components of the chimera.

AUTHOR INFORMATION

Corresponding Author

*E-mail: jayne.lawrence@kcl.ac.uk. Telephone: +44 (0) 207 848 4808. Fax: +44 (0) 207 848 4800.

ACKNOWLEDGMENT

F.F. is supported by an EPSRC "New Generation Facility Users" grant (EP/F021291/1) and gratefully acknowledges the provision of neutron beam time and the associated experimental support provided by staff of the STFC ISIS Large Scale Structures group.

REFERENCES

(1) Senior, J. H. *Crit. Rev. Ther. Drug Carrier Syst.* **1987**, *3*, 123–193.
(2) Lasic, D. D. *Liposomes: From Physics to Applications*; Elsevier: Amsterdam, 1993.
(3) Gregoriadis, G.; Davis, C. *Biochem. Biophys. Res. Commun.* **1979**, *89*, 1287–1293.
(4) Torchilin, V. P. *Nat. Rev. Drug Discovery* **2005**, *4*, 145–160.
(5) Phillips, M. C.; Johnson, W. J.; Rothblat, G. H. *Biochim. Biophys. Acta* **1987**, *906*, 223–276.
(6) Hamilton, J. A. *Curr. Opin. Lipidol.* **2003**, *14*, 263–271.
(7) Kan, C. C.; Yan, J.; Bittman, R. *Biochemistry* **1992**, *31*, 1866–1874.
(8) Huang, Z; Szoka, F. C., Jr. *J. Am. Chem. Soc.* **2008**, *130*, 15702–15712.
(9) Needham, D.; Evans, E. *Biochemistry* **1988**, *27*, 8261–8269.
(10) Kim, K.; Kim, C.; Byun, Y. *Langmuir* **2001**, *17*, 5066–5070.
(11) Kirby, C.; Gregoriadis, G. *Nat. Biotechnol.* **1984**, *2*, 979–984.
(12) Kotlarchyk, M.; Ritzau, S. M. *J. Appl. Crystallogr.* **1991**, *24*, 753–758.
(13) Shibayama, M.; Hashimoto, T. *Macromolecules* **1986**, *19*, 740–749.
(14) Skipper, N. T.; Soper, A. K.; McConnell, J. D. C. *J. Phys. Chem.* **1991**, *94*, 5751–5760.
(15) Ma, G.; Barlow, D. J.; Lawrence, M. J.; Heenan, R. K.; Timmins, P. *J. Phys. Chem. B* **2000**, *104*, 9081–9085.
(16) Harvey, R. D.; Heenan, R. K.; Barlow, D. J.; Lawrence, M. *J. Chem. Phys. Lipids* **2005**, *133*, 27–36.
(17) Harvey, R. D.; Barlow, D. J.; Drake, A. F.; Kudsiova, L.; Lawrence, M. J.; Brain, A. P. R.; Heenan, R. K. *J. Colloid Interface Sci.* **2007**, *315*, 648–661.
(18) Heenan, R. K. *RAL Report 89-129*, as subsequently revised; Rutherford Appleton Laboratory: Didcot, U.K., 1989.
(19) Morse, P. D.; Ma, L. D.; Magin, R. L.; Dunn, F. *Chem. Phys. Lipids* **1999**, *103*, 1–10.
(20) Petersen, N. O.; Kroon, P. A.; Kainosho, M.; Chan, S. I. *Chem. Phys. Lipids* **1975**, *14*, 343–349.
(21) Sunder, S.; Cameron, D.; Mantsch, H. H.; Bernstein, H. J. *Can. J. Chem.* **1978**, *56*, 2121–2126.
(22) Stottrup, B. L.; Keller, S. L. *Biophys. J.* **2006**, *90*, 3176–3183.
(23) Penfold, J.; Thomas, R. K. J. *J. Phys.: Condens. Matter* **1990**, *2*, 1369–1412.
(24) Greenwood, A. I.; Tristram-Nagle, S.; Nagle, J. F. *Chem. Phys. Lipids* **2006**, *143*, 1–10.
(25) Lu, J. R.; Thomas, R. K. *J. Chem. Soc., Faraday Trans.* **1998**, *94*, 995–1018.
(26) Hollinshead, C. M.; Harvey, R. D.; Barlow, D. J.; Webster, J. R. P.; Hughes, A. V.; Weston, A.; Lawrence, M. J. *Langmuir* **2009**, *25*, 4070–4077.
(27) Jendrasiack, G. L.; Smith, R. L. *Chem. Phys. Lipids* **2001**, *113*, 55–66.